Int. J. Heat Mass Transfer. Vol. 21, pp. 863–874
© Pergamon Press Ltd. 1978. Printed in Great Britain
0017-9310/78/0701-0863 $02.00/0

TRANSIENT HELIUM HEAT TRANSFER PHASE I—STATIC COOLANT*

W. G. STEWARD
Cryogenics Division, Institute for Basic Standards, National Bureau of Standards, Boulder, CO 80302, U.S.A.

(*Received* 24 *January* 1977 *and in revised form* 2 *January* 1978)

Abstract—Transient heat-transfer data have been obtained for flat heating surfaces in static liquid and supercritical helium. Measurements start $2(10)^{-5}$ s after step power inputs, and cover a heat flux range of 0.05–20 W/cm^2, pressures from 0.09–0.3 MPa, and four different heater orientations. Initial heat-transfer coefficients, being limited primarily by the Kapitza resistance, are 10–100 times greater than steady state, and the time to reach steady state varies from 10^{-5} to 1 s. For heat flux below the steady state peak nucleate boiling limit the temperature follows calculations based on pure conduction to the steady state nucleate boiling level. Above that limit the transient conduction period leads to an apparent metastable nucleation period followed by a transition to film boiling.

NOMENCLATURE

- c, heat capacity [j/g K];
- h, heat-transfer coefficient [W/cm^2 K];
- h_K, Kapitza conductance [W/cm^2 K];
- $h_{K,\mathrm{ref}}$, Kapitza conductance at T_{ref};
- K_f, thermal conductivity for the fluid [W/cm K];
- K_s, thermal conductivity for the substrate [W/cm K];
- P, power going into the fluid [W/cm^2];
- P_s, power going into the substrate [W/cm^2];
- T, temperature [K];
- T_{bath}, bath temperature [K];
- Z, coordinate normal to the heating surface [cm].

Greek symbols

- α_f, thermal diffusivity of the fluid [cm^2/s];
- α_s, thermal diffusivity of the substrate [cm^2/s];
- ΔT_f, temperature of the fluid above the bulk temperature [K];
- ΔT_s, temperature of the substrate above the bulk fluid temperature [K];
- θ, time from the start of a heating pulse [s];
- θ_P, duration of a pulse [s].

1. INTRODUCTION

MANY superconducting devices employ large power pulses or are subject to power transients due to overloads or other causes. It is usually desirable, and often imperative, that the superconductor does not quench during the pulse. In other cases one is concerned about the temperature recovery following heat release from flux jumps or micromechanical movements. Fortunately, heat transfer from the superconductor surface to the helium coolant can be many times higher during a short pulse than in steady state for a given surface temperature rise. Thus, even though rapid pulses or transients cause relatively high losses, the ability of the helium coolant to dissipate pulsed heat rapidly is a compensating factor.

At the beginning of a heating transient, as the power rises rapidly, the temperature gradient in the fluid adjacent to the solid surface may be extremely steep since a finite time is required for an equilibrium temperature field with less steep gradients to be established. During this period the thermal resistance is so low that Kapitza solid–liquid interface resistance, which is usually ignored at temperatures above the lambda point, may be the dominant resistance. Since nucleation, growth of bubbles, and formation of vapor films also require finite time, liquid exists at least briefly in non-equilibrium states above the saturation temperatures and boiling can be delayed significantly. As the thermal boundary layer thickens through prolonged application of power or repetition of pulses, convection effects become important and eventually steady state convection or boiling heat transfer are established. In a chain of pulses the surface temperature rises while the power is being applied and decays asymptotically toward the starting value while the power is off; therefore, the entire level of temperature rises with each pulse. The temperature ultimately reached after a large number of pulses is related to the average heat flux for the cycle and the steady state heat-transfer coefficient.

It is apparent that the use of steady state heat-transfer rates when designing for heating transients in superconducting devices is overly conservative. Yet, for lack of more appropriate data, steady state boiling helium heat-transfer data have been used in designs involving transient processes. An exception to the use of steady state data was the pulsed high energy inductive storage system designed by AERL [1] for the

*This work was carried out at the NBS Cryogenics Division, Boulder, CO under the sponsorship of the Air Force Office of Scientific Research, Washington, DC.

Air Force Aero Propulsion Laboratory. Heat flux for this design was estimated from the transient experimental data of Jackson [2]. This data is not sufficiently detailed, however, for general application. More recently, experimental results have been reported by two Japanese authors [3] at Yokohama National University, for the pulse heating of a thin lead film in a liquid helium bath. This study, however, gives only one point at the superconducting transition temperature of the lead film at a given power level, whereas, the entire temperature development is desired. The temperature rise after the onset of nucleate boiling until the establishment of steady temperatures has been experimentally determined by Bailey [4] at the Rutherford High Energy Laboratory, but the time scale was on the order of seconds and tenths of seconds and power densities were less than 25 mW/cm^2. In the wide range of existing and contemplated superconducting applications, pulses as brief as 0.05 ms and repetition rates as high as 200 per s are of concern [5]. In most applications, for economy of weight, material and liquid helium, the power levels will be pushed to the maximum safe limits as dictated by the ability of the coolant to dissipate heat due to transients, and these maximum heat fluxes may exceed 10 W/cm^2 for short pulses.

Therefore, it is clear that designers of superconducting equipment need a more complete picture of transient helium heat-transfer phenomena than was available before the commencement of this study. This total program will provide experimental data and verified predictive methods covering heat fluxes up to 25 W/cm^2, measurement times starting at less than 0.05 ms extending to steady state, varying orientation of the heated surfaces, varying helium pressures and temperatures, and both static and forced flow of coolant. This paper covers the first phase of the program, namely the experimental results for a static coolant.

2. IDEALIZED TRANSIENT CONDUCTION HEAT TRANSFER

At the beginning of a heating transient, before convection currents or boiling have been established, conduction is the principle mechanism of heat transfer. The following set of assumptions and boundary conditions for solution of the heat-conduction equation apply to the configuration of the test apparatus.

1. The heat source is an infinite plate in the X–Y plane at $Z = 0$. (This is equivalent to assuming that the thermal boundary layer is very thin relative to the width of the plate.)
2. Heating occurs only on the surface at the liquid–solid interface.
3. Stagnant liquid helium is present at $Z > 0$.
4. A solid substrate exists at $Z < 0$.
5. Time during which heat is applied is short enough that convection currents are not established. This means there is not time for bubble formation and temperatures may exceed the equilibrium saturation temperature.
6. Radiation heat transfer is negligible.
7. Fluid and solid properties are constant.
8. Temperature difference due to Kapitza resistance may be considered separately.

The Fourier heat-conduction equation in one dimension of the solid substrate is [6],

$$\frac{\partial^2 \Delta T_s}{\partial Z^2} = \frac{1}{\alpha_s}\frac{\partial \Delta T_s}{\partial \theta}, \quad Z \leq 0; \tag{1}$$

and for the fluid

$$\frac{\partial^2 \Delta T_f}{\partial Z^2} = \frac{1}{\alpha_f}\frac{\partial \Delta T_f}{\partial \theta}, \quad Z > 0. \tag{2}$$

Boundary conditions for the substrate for a square wave heat pulse are,

$$\Delta T_s(Z, 0) = 0 \tag{3}$$

$$\lim_{Z \to -\infty} \Delta T_s(Z, \theta) = 0 \tag{4}$$

$$P_s = K_s\left(\frac{\partial \Delta T_s}{\partial Z}\right)_{0,\theta}, \quad 0 < \theta < \theta_p \tag{5}$$

$$P_s = 0, \quad \theta > \theta_p.$$

P_s is the part of the heater power being dissipated in the substrate. Boundary conditions for the fluid are,

$$\Delta T_f(Z, 0) = 0 \tag{6}$$

$$\lim_{Z \to \infty} \Delta T_f(Z, \theta) = 0 \tag{7}$$

$$P_f = -K_f\left(\frac{\partial \Delta T}{\partial Z}\right)_{0,\theta}, \quad 0 < \theta < \theta_p \tag{8}$$

$$P_f = 0, \quad \theta > \theta_p.$$

P_f is the part of the heater power being dissipated in the fluid. Also, the total heater power is

$$P = P_f + P_s \tag{9}$$

where

$$P = \text{constant} \quad 0 < \theta < \theta_p, \qquad P = 0 \quad \theta \geq \theta_p,$$

and

$$\Delta T_s(0, \theta) = \Delta T_f(0, \theta). \tag{10}$$

The solution for the fluid is [6],

$$\Delta T_f = \frac{P_f}{K}\left\{2\left(\frac{\alpha_f \theta}{\pi}\right)^{1/2} \exp\left(\frac{-Z^2}{4\alpha_f \theta}\right) - Z\,\text{erfc}\left|\frac{Z}{2(\alpha_f \theta)^{1/2}}\right|\right\} \quad \text{for} \quad 0 < \theta < \theta_p \tag{11}$$

and

$$\Delta T_f = \frac{P_f}{K_f}\left\{2\left(\frac{\alpha_f \theta}{\pi}\right)^{1/2} \exp\left(\frac{-Z^2}{4\alpha_f \theta}\right) - Z\,\text{erfc}\left|\frac{Z}{2(\alpha_f \theta)^{1/2}}\right|\right\}$$
$$-\frac{P_f}{K_f}\left(2\left|\frac{\alpha_f(\theta - \theta_p)}{\pi}\right|^{1/2} \exp\left|\frac{-Z^2}{4\alpha_f(\theta - \theta_p)}\right| - Z\,\text{erfc}\left\{\frac{Z}{|2[\alpha_f(\theta - \theta_p)]^{1/2}|}\right\}\right) \quad \text{for} \quad \theta > \theta_p. \tag{12}$$

The equations for the substrate temperature field are exactly analogous to (11) and (12) except that a subscript "s" appears instead of "f".

At the surface ($Z = 0$) we have

$$\Delta T_f(0,\theta) = \frac{2P}{(\pi)^{1/2}} \frac{(\theta)^{1/2}}{\left[\frac{K_s}{(\alpha_s)^{1/2}} + \frac{K_f}{(\alpha_f)^{1/2}}\right]}, \qquad 0 < \theta < \theta_P \tag{13}$$

and

$$\Delta T_f(0,\theta) = \frac{2P}{(\pi)^{1/2}} \frac{[(\theta)^{1/2} - (\theta-\theta_P)^{1/2}]}{\left[\frac{K_s}{(\alpha_s)^{1/2}} + \frac{K_f}{(\alpha_f)^{1/2}}\right]}, \qquad \theta > \theta_P. \tag{14}$$

Equation (13) gives the surface temperature rise during the heat pulse and equation (14) gives the temperature decay following the pulse.

Obviously the assumptions drastically limit the time during which equations (13) and (14) are valid. Comparison with experimental data help determine the conduction period duration.

3. KAPITZA RESISTANCE

Whereas fluid thermal resistance builds up as the boundary layer develops, Kapitza resistance apparently occurs the instant heat flow begins. Consequently, Kapitza resistance initially dominates the heat flow process at liquid helium temperatures, though only briefly. How long Kapitza resistance dominates depends upon its magnitude in relation to the increasing conduction resistance, and this in turn depends on the kind of material and physical condition of the surface as well as the temperature.

Since the exact nature of a surface is difficult to characterize [7] and may change with time, the influence of material and surface condition is difficult to predict. However, for a given heater the Kapitza conductance h_K (reciprocal of resistance) has been observed to obey approximately a T^3 relationship [7]:

$$h_K = \frac{P_f}{\Delta T_K} = h_{K,\mathrm{ref}}\left(\frac{T}{T_{\mathrm{ref}}}\right)^3, \tag{15}$$

where $h_{K,\mathrm{ref}}$ is a constant Kapitza conductance at reference temperature T_{ref}, P_f is the power being dissipated into the helium bath.

The heater surface temperature is

$$T = T_{\mathrm{bath}} + \Delta T_f + \Delta T_K.$$

Therefore,

$$P = \frac{h_{K,\mathrm{ref}}}{T_{\mathrm{ref}}^3}(T_{\mathrm{bath}} + \Delta T_f + \Delta T_K)^3 \Delta T_K. \tag{16}$$

For low power levels ΔT_K can be estimated from the experimental data as the asymptote of the temperature curve as $\theta \to 0$. In this way it was determined that

$$h_K = 0.7\ \mathrm{W/cm^2\,K} \text{ at approximately } 4\ \mathrm{K}.$$

Also,

$$\frac{h_{K,\mathrm{ref}}}{T_{\mathrm{ref}}^3} = 0.011 \frac{\mathrm{W}}{\mathrm{cm^2\,K^4}}. \tag{17}$$

If $T_{\mathrm{ref}} - 1.9\ \mathrm{K}$, $h_{K,\mathrm{ref}} = 0.075$ which is well within the possible range of values of h_K at 1.9 K shown by Snyder [7].

4. EXPERIMENTAL PROGRAM

The apparatus used is shown schematically in Fig. 1. A carbon thin film resistor [8] whose resistance is a known function of temperature serves both as an extremely fast response heater and thermometer. Its dimensions are approximately 5 mm parallel to current by 10 mm wide. The carbon film is deposited on a quartz substrate which has an extremely low heat capacity at liquid helium temperature so that most of the heat flows into the fluid and very little flows into the substrate. Voltage across the film and voltage across a standard resistor are recorded at intervals as close as 0.5 μs by a digital recording oscilloscope; 2048 points are recorded on each sweep of the oscilloscope on each of two channels. Power may be supplied as a

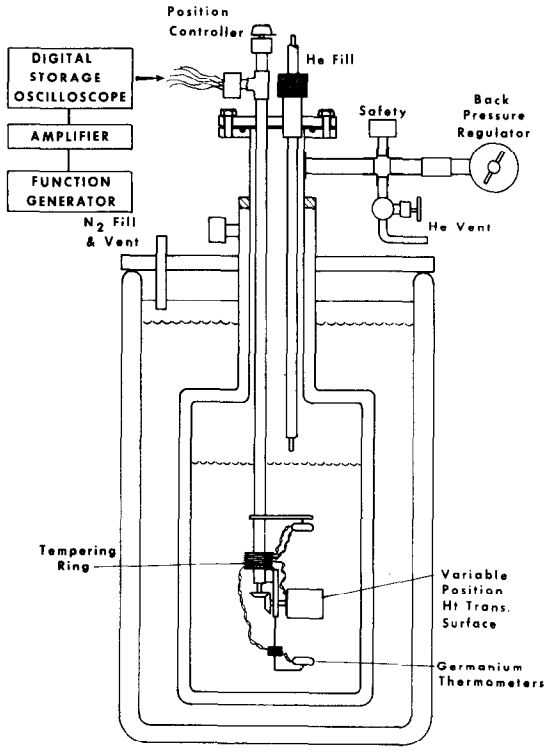

FIG. 1. Pool pulsed heat-transfer experimental apparatus.

step function or as pulses of any desired width or frequency. A minicomputer data acquisition system has been added to facilitate data processing and to permanently record the data. The heater surface temperature, power level and heat-transfer coefficients are printed as a function of time.

For these tests the heater was submerged in a static helium bath. Insofar as possible power was applied as a step input or square wave pulse and ramp times of less than 1.5×10^{-5} s were achieved. However, at high power levels resistance change due to large temperature rise causes power variation of up to $\pm 10\%$ from the average. Tests covered the following parameter variations:

1. Power densities ranging from 0.05–20 W/cm^2 repeated for each variation of the other parameters.
2. Four orientations of the heater—vertical, horizontal facing up, horizontal facing down, and 45° down.
3. Variations in bath pressure and temperature.
4. Repetition of square wave pulses with variations of pulse width and time between pulses. Finally, temperature decays following single pulses were recorded.

4.1. *Preliminary liquid nitrogen transient heat-transfer experiments*

We performed tests at four power levels with liquid nitrogen for a check on measurement techniques and predictions for a fluid which is markedly different from helium in heat transfer related properties, and for which Kapitza resistance is negligible. Figure 2 shows the temperature rise of a vertical heater surface in liquid nitrogen as a function of time from the start of a step power input. The heat flux per unit area was nearly constant during the measurements and the four tests were at 5, 10, 15 and 18 W/cm^2. The temperature rise in the first 3×10^{-2} s closely follows the non-boiling transient heat-transfer calculations.

For 5, 10 and 15 W/cm^2 the heater temperature continued to rise in proportion to (time)$^{1/2}$ and for 9–15 K above the steady state nucleate boiling level, then dropped back down to that level. The time required to finally reach steady state nucleate boiling was approximately 0.2 s. A power density of 18 W/cm^2 exceeded the maximum nucleate boiling heat flux and the heater began a slow transition to a film boiling temperature which might have burned out the heater if the heating had been allowed to continue.

The heater temperature rise during the non-boiling transient heat-transfer period was calculated from equation (13) in which

$$\frac{K_s}{(\alpha_s)^{1/2}} + \frac{K_f}{(\alpha_f)^{1/2}} = 0.0906 \frac{\mathrm{W\,s^{1/2}}}{\mathrm{cm^2\,K}} \text{ for } LN_2$$

and quartz substrate. At liquid nitrogen temperature Kapitza resistance is negligible; therefore $\Delta T = \Delta T_f$.

4.2. *Liquid helium transient heat-transfer experiments with a vertical heater*

4.2.1. *Accuracy.* The carbon thermometer resistance at helium temperature increased by 1.3% over the duration of the test program; however, this slow drift did not affect the test results since the thermometer was calibrated at room temperature and by nitrogen and helium vapor pressure measurements each time the apparatus was cooled from room temperature and the

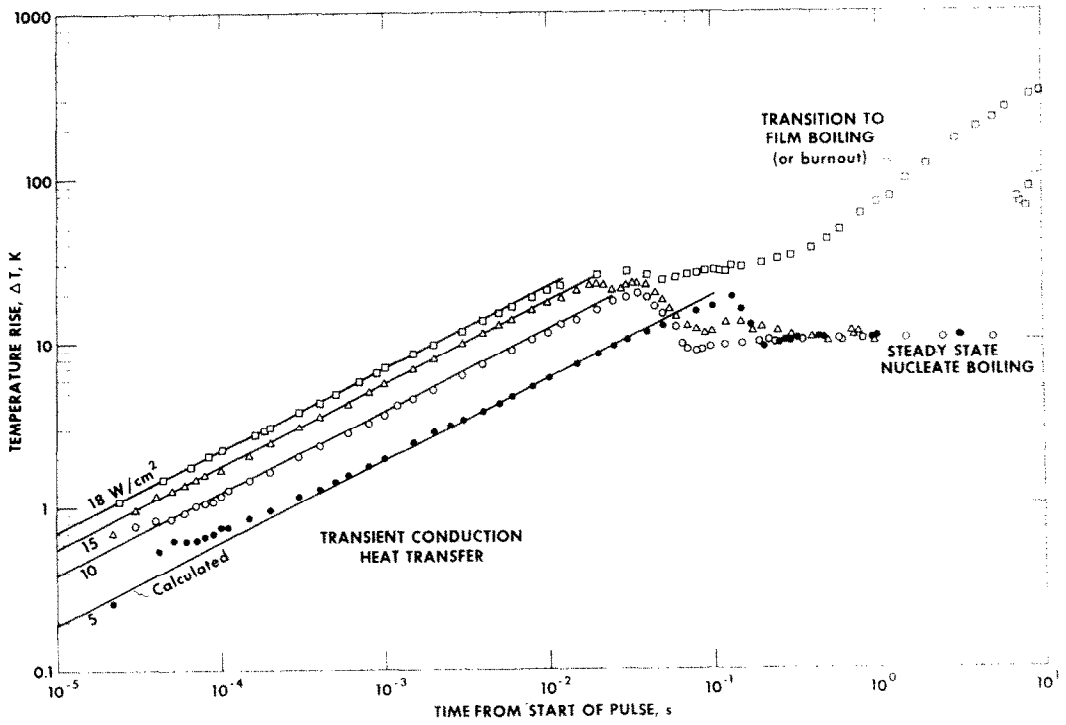

FIG. 2. Transient heat transfer from a vertical heater to liquid nitrogen.

helium temperature calibration was re-established before each test. Systematic error in calibration is no more than ± 0.01 K, and experience with pulses repeated seconds apart and months apart indicate that heater-to-bath temperature difference measurements were repeatable within $\pm 5\%$. While instantaneous heater power is accurate to $\pm 0.1\%$, the variation during a pulse from the stated average power due to heater resistance change ranges from $\pm 1\%$ at 0.1 W/cm^2 to a maximum of $\pm 8\%$ at 20 W/cm^2. Time measurements are initiated by the triggering of the digital oscilloscope at the beginning of a pulse; however, the time to achieve essentially steady power is approximately 5 μs later than the triggering time. No corrections were made in the plotted data for the finite power rise time.

The liquid helium results are complicated by a significant Kapitza resistance which is added in series with the thermal boundary-layer resistance. Because of the Kapitza resistance the heater temperature does not rise simply in proportion to $(\theta)^{1/2}$ during the non-boiling transient heat-transfer period. For helium

$$\Delta T = \Delta T_K + \Delta T_f,$$

where ΔT_f is given by equation (13). For helium the quantity

$$\frac{K_s}{(\alpha_s)^{1/2}} + \frac{K_f}{(\alpha_f)^{1/2}} = 0.0118 \frac{\text{W s}^{1/2}}{\text{cm}^2\,\text{K}}. \qquad (18)$$

The surface temperature step ΔT_K due to Kapitza resistance is given by equation (15).

The non-boiling transient heat-transfer calculations using equations (13), (2), (3) and the constant (4) are shown in Fig. 3. The earliest time at which temperature can be measured is about 20×10^{-6} s. It can be seen that except at low power levels the non-boiling transient heat-transfer period is over by 20×10^{-6} s; however, the calculated temperatures at $\theta < 20 \times 10^{-6}$ s are consistent with the measured temperatures. The non-boiling transient period leads either to steady state nucleate boiling as in the 0.1–0.6 W/cm^2 curves or to a metastable nucleation period at higher power levels. The length of time the metastable nucleation period lasts decreases as the power level increases. (The steady state nucleate boiling at power levels below 0.6 W/cm^2 might be thought of as a "metastable" nucleation period which lasts indefinitely.) At power levels of 1 W/cm^2 and above, the metastable nucleation period leads to a period of relatively slow transition to stable film boiling. At the highest power levels of 9, 15 and 25 W/cm^2 the transition to film boiling has already begun at the earliest possible measurement times. The transition times become longer at higher power so that steady state film boiling is reached at about 0.1 s for all power levels.

The steady state nucleate and film boiling power level vs temperature rise relationships are shown along with data from previous research [9] in Fig. 4. The new data, including the value of the peak steady state nucleate boiling heat flux, compares well with the previous data and Kutateladze correlation but with nucleate boiling ΔT slightly on the high side. It is interesting to note that the metastable nucleation data falls on an extension of the nucleate boiling curve above the steady state peak heat flux. The curve of Kapitza ΔT_K vs P is also shown on this curve. Obviously the nucleate boiling ΔT must be greater than ΔT_K, so the very large Kapitza resistance of the carbon film may account for the slightly higher than average nucleate boiling ΔT of the new data.

Heat-transfer coefficients derived from these data are discussed in Section 4.6.

4.3. *The effect of heater orientation on transient helium heat transfer*

The orientation of the heating surface is known to be an important factor in steady state natural convection

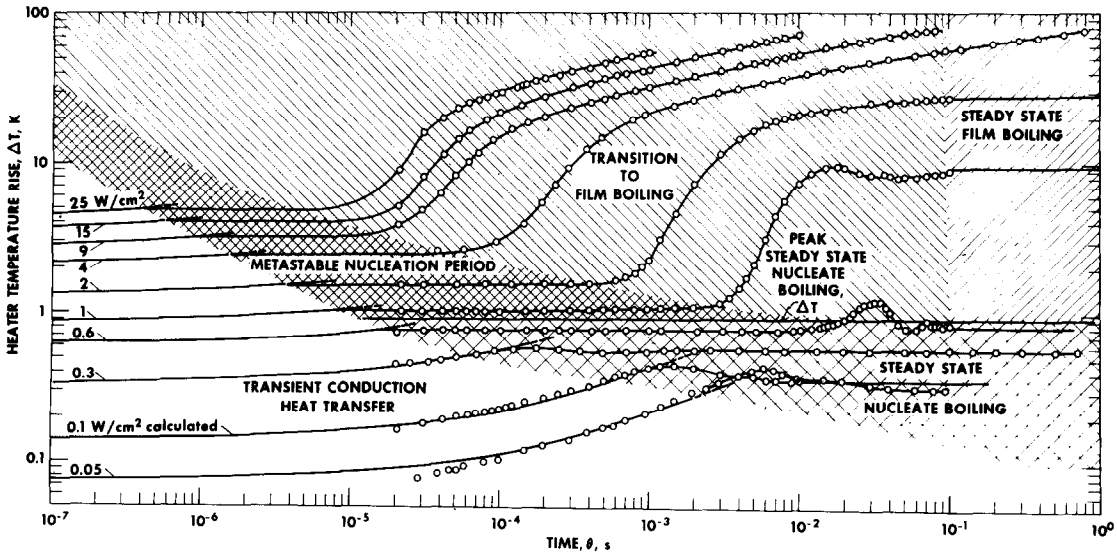

FIG. 3. Transient heat transfer to a saturated liquid helium bath at 4 K from a vertical heater.

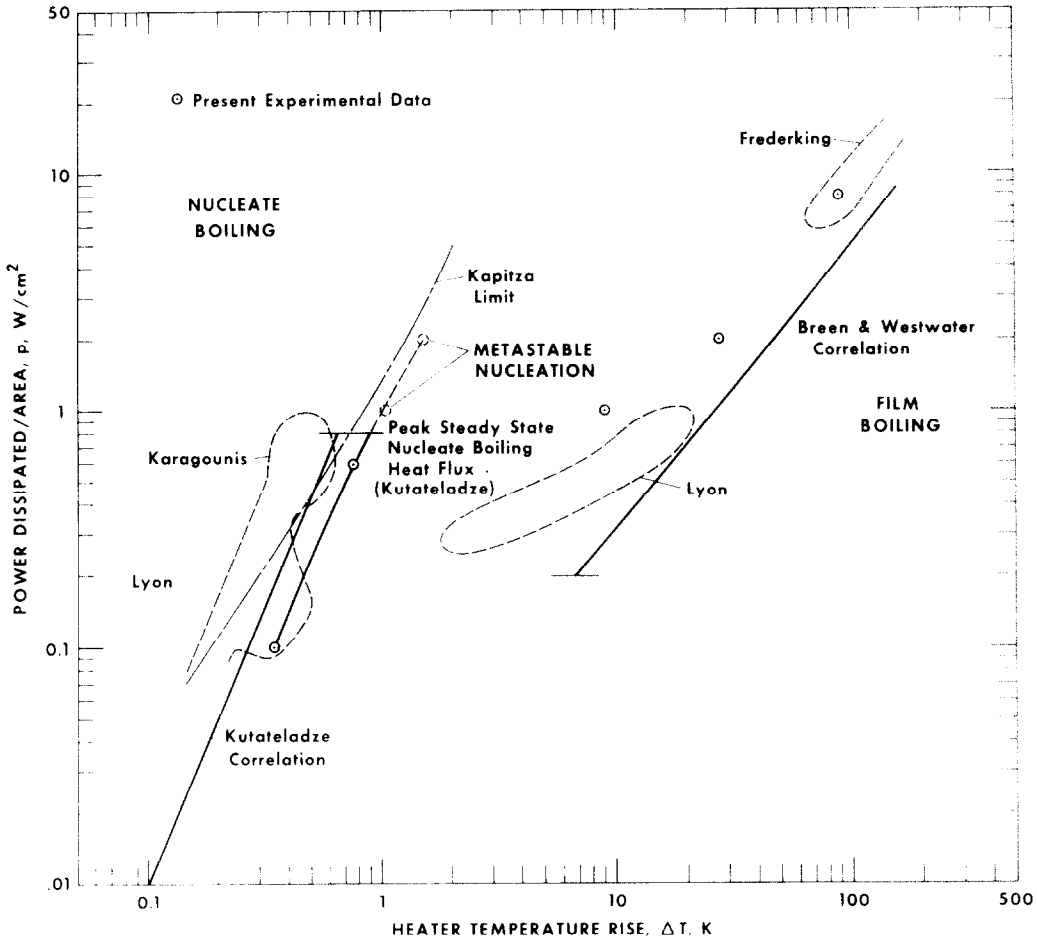

FIG. 4. Comparison between the present experimental data in steady state boiling and previous research as discussed in [9].

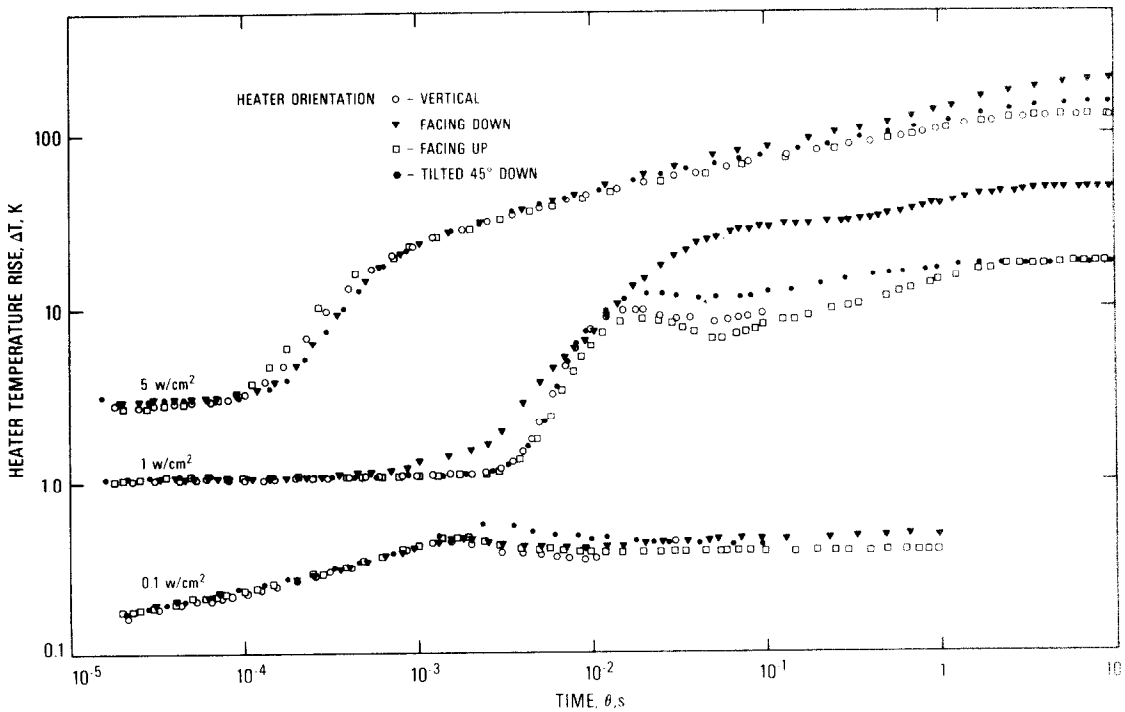

FIG. 5. Comparison of heater temperature rise for the four orientations.

and boiling heat transfer because of the effect of buoyancy and orientation in inducing currents and in expelling vapor bubbles. Particularly in boiling, bubbles formed on a vertical or upward facing surface tend to be expelled and swept away; whereas, bubbles forming on a downward facing surface tend to be trapped and form a thick insulating film which results in poorer cooling. Data such as shown in Fig. 3 for the vertical heater have been obtained for the horizontal facing up, facing down, and 45° facing down positions. Comparisons are shown in Fig. 5 for power levels of 0.1 W/cm^2 in the steady state nucleate boiling regime, and 1.0 and 5 W/cm^2 in the film boiling regime. Little effect of orientation is seen in the transient regime; however, the downward facing heater finally rose markedly above the other orientations particularly in steady state film boiling. The effect is less pronounced in the nucleate boiling range but still exists there. In general, vertical and horizontal facing up positions are nearly the same; 45° tilted downward gives the medium temperature, and a heater facing straight down produces the highest temperatures.

4.4. *Pressure effects*

In all tests of Fig. 6 the bath bulk temperature was maintained at approximately 4.02 K; the pressure is raised to 0.151 MPa (▲ symbol) and 0.310 MPa (□ symbol) as opposed to atmospheric pressure, 0.086 MPa (○ symbol). For a heat flux of 0.1 W/cm^2 the temperatures for the three pressures follow nearly the same transient conduction curve; however, the higher pressures lead to decidedly higher steady state temperatures as would be expected; the increase in surface temperature in going from 0.086–0.151 MPa is approximately the same as the increase in saturation temperature between those pressures. It should be noted that the highest pressure, 0.310 MPa is above the critical pressure, yet the steady state temperature is consistent with the boiling curves lower pressures. The same phenomena can be seen in the metastable nucleation region to the left of the transition to film boiling at 1 and 5 W/cm^2. However, at 0.310 MPa the transient conduction curve leads directly to the transition to film boiling with no period of apparent nucleation. At 5 W/cm^2 only a small flat region can be observed at times less than 10^{-4} s for 0.086 MPa, and the two higher pressures are already in transition to film boiling at the earliest measured time.

It is interesting that the trend of steady state film boiling temperatures at 5 W/cm^2 is reversed from that of nucleate boiling. This is perhaps due to improved heat transfer through the vapor or supercritical fluid film at higher pressure and that the film would be thinner at higher pressure. This does not explain the behavior at 1 W/cm^2 in which the highest pressure produces the highest temperature as in nucleate boiling. However, the fact that the steady state heat transfer at 1 W/cm^2 exhibits some characteristics of nucleate boiling is not particularly disturbing since then heat flux is only slightly above the nucleate boiling peak and some regions of the surface are probably undergoing nucleate boiling.

4.5. *Repetition of pulses and temperature decay*

When heating pulses are repeated the temperature rises while the power is being applied and decays

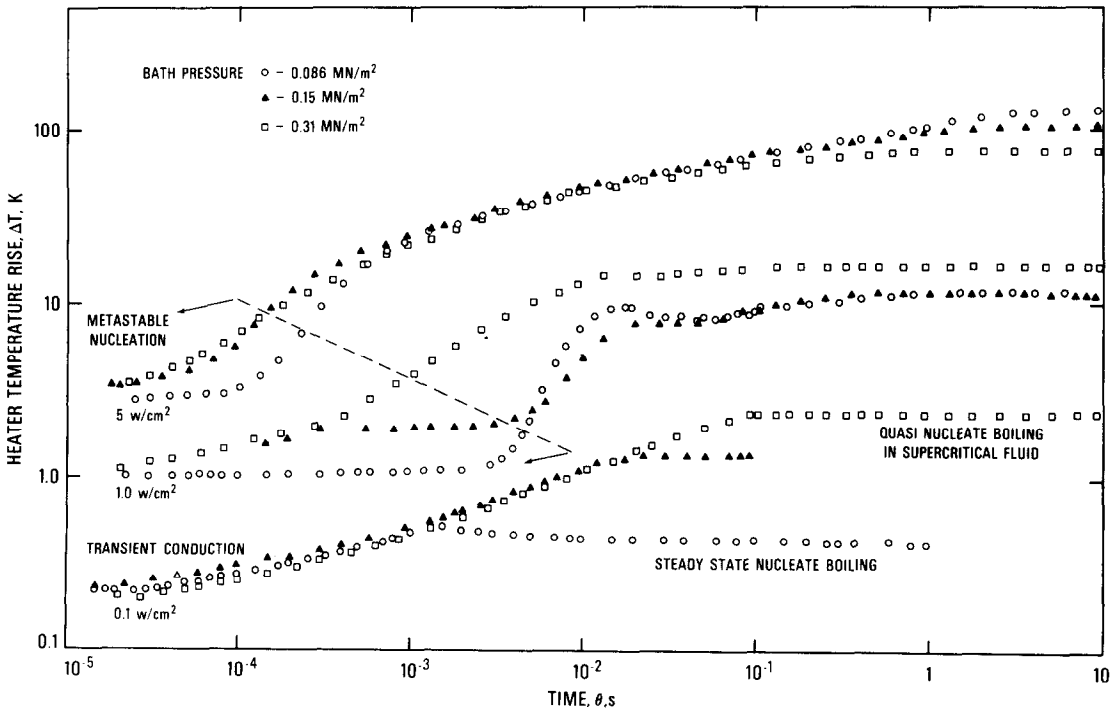

FIG. 6. Effect of bath pressure on the temperature history for a vertical heater in 4 K liquid and supercritical helium.

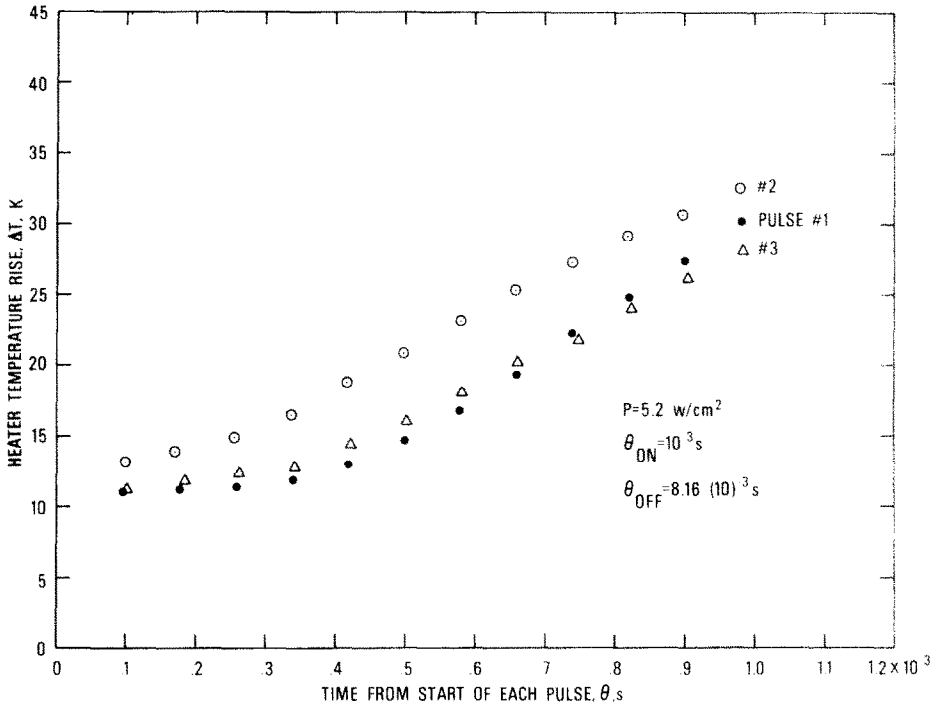

FIG. 7. Temperature rise during repeated square wave pulses of 5.2 W/cm^2 for a pulse duration of 10^{-3} s and 8.16×10^{-3} s between pulses.

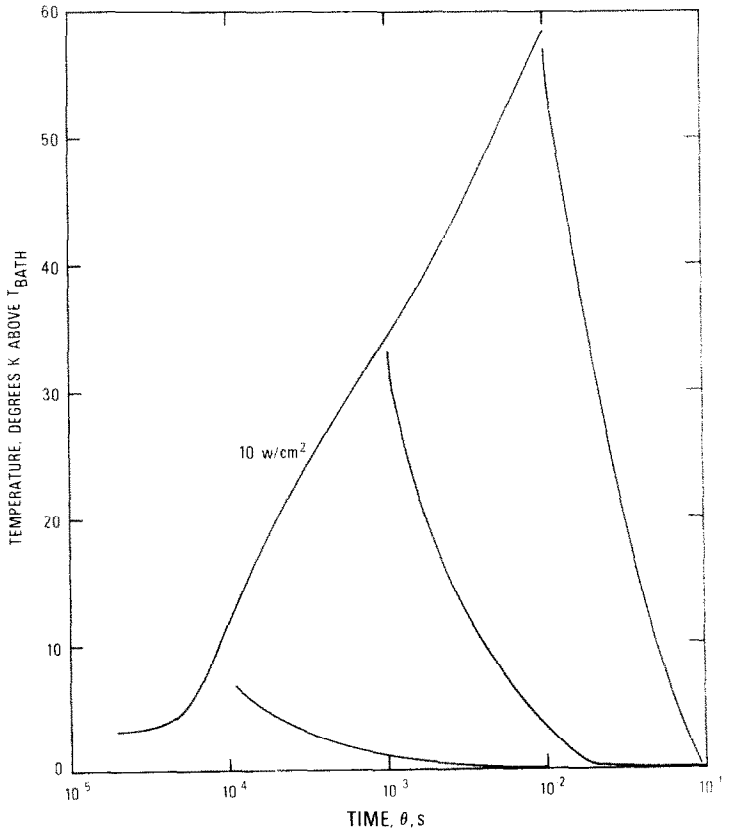

FIG. 8. Temperature decay following 10 W/cm^2 pulses of 10^{-4}, 10^{-3} and 10^{-2} s duration.

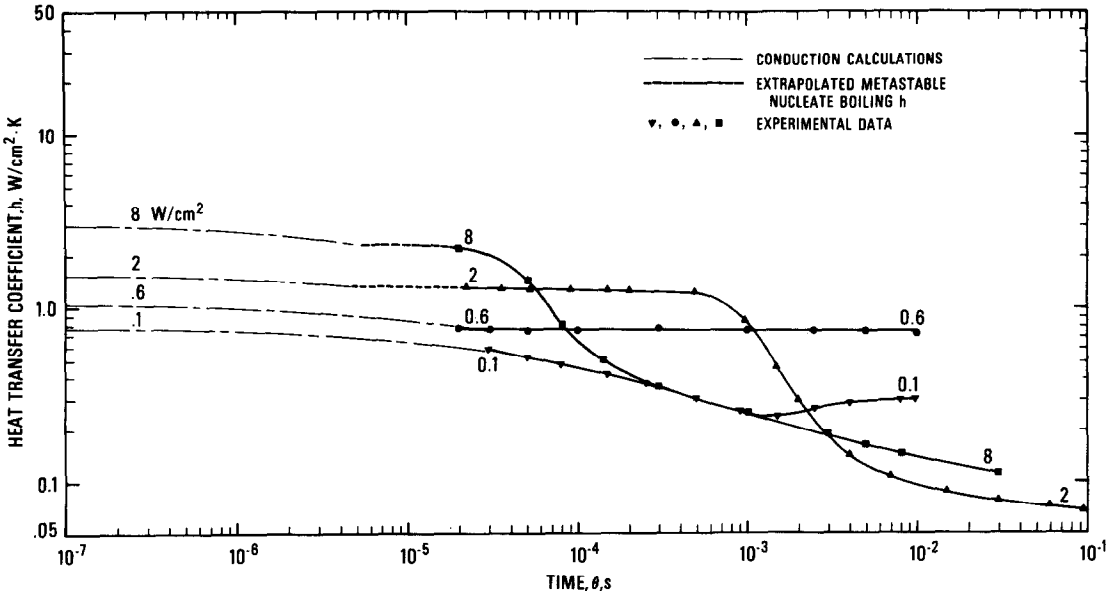

FIG. 9. Transient heat-transfer coefficients for a vertical carbon film heat transfer surface in saturated liquid helium at 4 K.

asymptotically toward the bath temperature while the power is off. If succeeding pulses begin before the surface has fully regained equilibrium with the bulk fluid the entire level of temperature rises with each pulse until a stable condition is reached in which the total energy of each pulse is dissipated during each cycle. Figure 7 is an example of one of these temperature histories during 1 ms heating pulses of 5.2 W/cm^2 and an off-time of 8.16×10^{-3} s. These tests show, for this example, that sustained pulses would produce a peak temperature of approximately 30 K above the bath temperature.

Figure 8 shows a typical temperature decay following square wave heat pulses. The nature of these decay curves depends on not only the heat flux during the pulse but on the temperature reached at the end of the pulse and the duration of the pulse. All of these factors affect the boundary-layer temperature profile as the decay begins. These figures confirm the previous interpretation of the initial temperature step as being due to Kapitza resistance. Following the pulse, when the power is essentially removed (except for a small measurement current) and Kapitza resistance should disappear, the temperature does in fact return to the bath temperature.

4.6. *Heat-transfer coefficients*

Heat-transfer coefficients were calculated for all of the experimental data. Some of these are shown in Fig. 9 for a vertical heater and atmospheric pressure, along with curves calculated from,

$$h = \frac{P_f}{(\Delta T_f + \Delta T_K)} \tag{19}$$

where ΔT_f and ΔT_K are from equations (13) and (17).

At the lowest power levels of 0.051 and 0.1 W/cm^2 the experimental data is seen to follow the transient calculations until steady state nucleate boiling is reached. The steady state condition is preceeded in both those cases by a dip in heat-transfer coefficient corresponding to the slight temperature overshoot seen in Fig. 3. It is seen that the time to reach steady state varies all the way from 10^{-5} to 1 s.

At 0.6 W/cm^2 a vestige of the transient curve is seen just before nucleate boiling begins at about 3×10^{-5} s; however, at higher power levels transient conduction curves apparently intersect the boiling or metastable boiling curves before the earliest measurement time. The extrapolation of the metastable nucleation curves for 2 and 8 W/cm^2 to the transient conduction intersections are shown in dashed lines in Fig. 9. It should be emphasized that the extrapolated curves are rough estimates.

The Kapitza resistance of the carbon heat-transfer surface may be representative of materials used for insulation but is considerably higher than typical base metals. The heat-transfer coefficients for heaters with negligible Kapitza resistance have been estimated by subtracting ΔT_K from equation (17) from the observed ΔT. The transient conduction heat-transfer coefficient then becomes independent of P. The significance of the Kapitza resistance at the carbon surface may be seen by comparison of heat-transfer coefficients in Figs. 9 and 10. Due to the T^3 relationship (equation 15) the effect of Kapitza resistance is pronounced at early times, before the surface temperature has risen significantly, but virtually disappears in steady state.

Negligible Kapitza-resistance heat-transfer coefficients such as shown in Fig. 10 are compared with the experimental data of Jackson [2] in Fig. 11. The 0.031 cm manganin wire used as heater and thermometer by Jackson may account for the rather large differences between the two sets of data since surface curvature has a pronounced effect on bubble nuc-

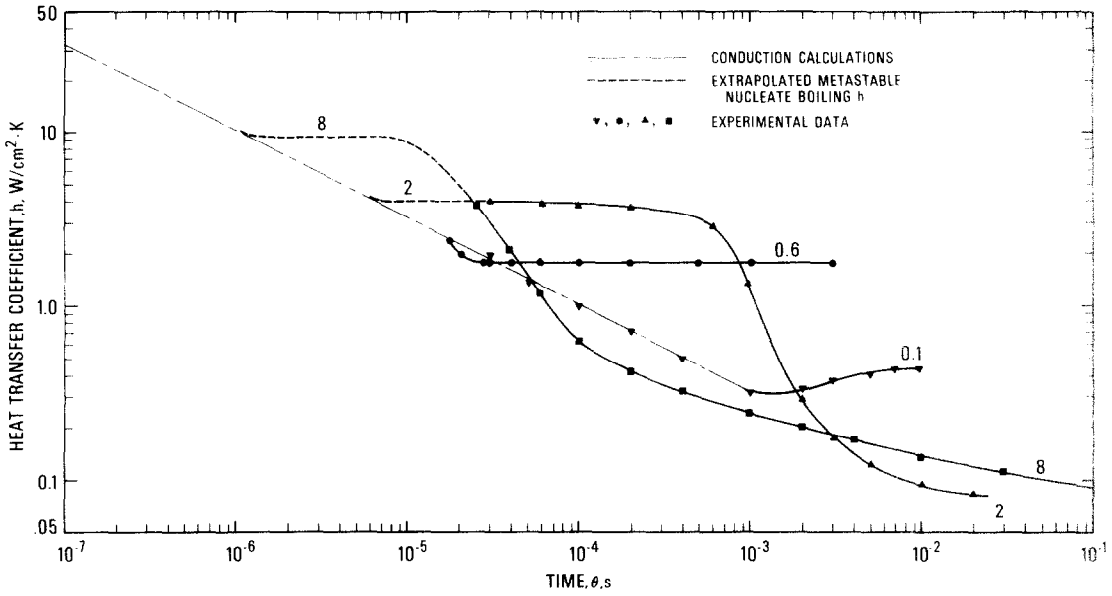

FIG. 10. Transient heat-transfer coefficients for a heat-transfer surface having negligible Kapitza resistance.

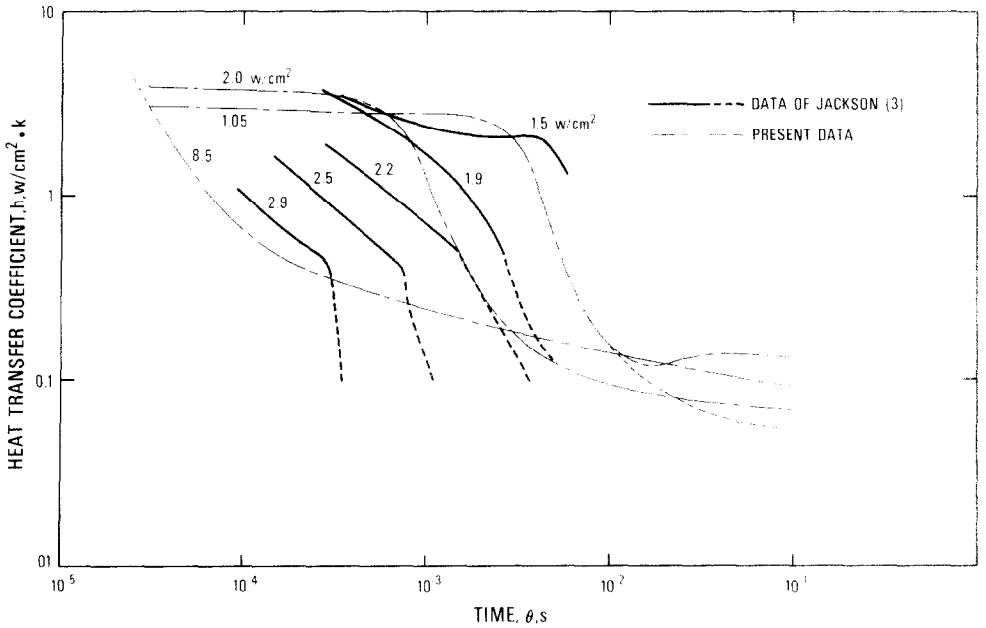

FIG. 11. Comparison between the heat transient heat-transfer coefficient data of Jackson [3] and the present data.

leation when the radius of curvature is on the order of the bubble radii. Even though there are points of agreement on the curves of 1.5–2.2 W/cm² the slope $dh/d\theta$ is considerably steeper in the present data and Jackson's data indicates larger dependence of h on heat flux.

5. CONCLUSIONS

Transient heat-transfer experiments using fast response carbon thin film heater thermometers in a static helium bath show the effects of heat flux, heater orientation and pressure on surface temperature and heat-transfer coefficients. For heat flux below the steady state peak nucleate boiling limit the surface temperatures follow calculations based on pure conduction (allowing for Kapitza resistance) until, after a small overshoot, the temperature reaches the steady state nucleate boiling level. Above the steady state nucleate boiling peak the transient conduction period leads to an apparent metastable nucleate boiling period followed by a transition to film boiling. All of these events vary systematically with heat flux. Steady state temperatures fall within the range of previous experimental data which, granted, allows considerable latitude.

A downward facing orientation of the heater increases the steady state temperature rise 20–60%, over the other orientations, but has little effect during

transients. Likewise, raising the coolant helium pressure has little effect during the transient conduction period but raises the steady state and metastable nucleate boiling temperature levels. The effect of pressure is reversed in steady state film boiling, apparently because increased pressure improves heat transfer through the vapor (or low density supercritical fluid) film.

Kapitza resistance for materials such as the carbon heat-transfer surface used in these experiments may override much of the benefit which might have been gained from the initial high helium conduction heat transfer. For that reason the type of electrical insulating material or metal covering the superconductor and contacting the helium coolant will have a significant effect on transient cooling. Investigation of surface material effects as well as forced convection effects are planned for a continuation of this program.

Steady state nucleate boiling is reached in 10^{-5}–10^{-2} s, but steady state film boiling conditions are not reached until 10^{-1}–1 s from the beginning of a heat pulse. Since the initial heat flux is at least an order of magnitude higher than steady state, the time variations in heat-transfer coefficients should be considered in the design and analysis of superconducting equipment if these transition times comprise a significant part of anticipated heating pulses.

Acknowledgements—The author wishes to acknowledge the contributions of Dr. M. C. Jones who recognized the need for helium transient heat-transfer data and supplied many of the ideas for measurement methods. Thanks are due also to Dr. Vincent Arp for many helpful suggestions and preliminary studies.

REFERENCES

1. J. Teno, O. K. Sonju and L. M. Lontai, Development of a pulsed high-energy inductive energy storage system, Final Report, AVCO Everett Research Laboratory, Inc. prepared for Air Force Aero Propulsion Laboratory, Wright–Patterson Air Force Base (1973).
2. J. Jackson, Transient heat transfer and stability of superconducting composites, *Cryogenics* **9**, 103 (1969).
3. O. Tsukamoto and S. Kobayashi, Transient heat transfer characteristics of liquid helium, *J. Appl. Phys.* **46**(3), 1359–1364 (1975).
4. R. L. Bailey, Heat transfer to liquid helium in pulsed heated channels, Experiment Report RL-73-089, Department of Engineering Science, Rutherford High Energy Laboratory, Chilton Didcot Berkshire, England (1973).
5. V. Arp, P. J. Giarratano, R. C. Hess and M. C. Jones, Heat transfer in pulsed superconducting magnets, Nat. Bur. Stand. (U.S.) NBSIR 74-363 (1974).
6. H. S. Carslaw and J. C. Jaeger, *Conduction of Heat in Solids*, Oxford University Press, Oxford (1950).
7. N. S. Snyder, Thermal conductance at the interface of a solid and helium II (Kapitza conductance), Nat. Bur. Stand. (U.S.) Tech. Note 385 (1969).
8. R. S. Collier, L. L. Sparks and T. R. Strobridge, Carbon thin film thermometry, Nat. Bur. Stand. (U.S.) NBSIR 74-355 (1973).
9. E. G. Brentari, P. J. Giarratano and R. V. Smith, Boiling heat transfer for oxygen, nitrogen, hydrogen and helium, Nat. Bur. Stand. (U.S.) Tech. Note 317 (1965).

TRANSFERT THERMIQUE TRANSITOIRE DANS L'HELIUM PHASE I—REFRIGERANT STATIQUE

Résumé—On donne des résultats concernant le transfert thermique variable pour des surfaces planes et chaudes dans de l'hélium supercritique et statique. Les mesures commencent $2(10)^{-5}$ s après un échelon de puissance et elles couvrent des domaines de flux entre 0,05 et 20 W/cm^2 et de pression entre 0,09 et 0,3 M Pa, pour quatre orientations différentes du chauffoir. Les coefficients de transfert thermique initiaux, étant limités par la résistance de Kapitza, sont 10 et 100 fois supérieurs à ceux du régime permanent et le temps pour atteindre le régime permanent varie de 10^{-5} à 1 s. Pour un flux thermique au dessous de la limite du pic d'ébullition nucléée en régime permanent, la température suit les calculs basés sur la conduction pure au niveau de l'ébullition nucléée permanente. Au dessus de cette limite, la période de conduction variable conduit à une période de nucléation métastable apparente suivie par une transition à l'ébullition en film.

INSTATIONÄRE WÄRMEÜBERTRAGUNG AN HELIUM PHASE I—STATIONÄRES KÜHLMITTEL

Zusammenfassung—An ebenen Heizflächen wurde in ruhender Flüssigkeit und überkritischem Helium die instationäre Wärmeübertragung gemessen. Die Messungen beginnen $2 \cdot 10^{-5}$ s nach dem sprunghaften Anlegen der Spannung und überdecken einen Wärmestrombereich von 0,05 bis 20 W/cm^2, Drücke von 0,09 bis 0,3 MPa und vier verschiedene Heizplattenausrichtungen. Anfängliche Wärmeübertragungskoeffizienten, die zuerst durch den Kapitza-Widerstand begrenzt werden, sind 10 bis 100 mal größer als im stationären Zustand, und die Zeit, die es dauert, den stationären Zustand zu erreichen, variiert von 10^{-5} s bis 1 s. Bei Wärmeströmen unterhalb der Obergrenze für stationäres Blasensieden stellen sich Temperaturen ein, die bis zum Punkt des stationären Blasensiedens den Berechnungen für reine Wärmeleitung folgen. Über diesem Punkt geht die instationäre Wärmeleitung in offensichtlich metastabiles Blasensieden über, dem der Übergang zum Filmsieden folgt.

НЕСТАЦИОНАРНЫЙ ТЕПЛООБМЕН В ГЕЛИИ I. НЕПОДВИЖНЫЙ ХЛАДАГЕНТ

Аннотация — Данные по нестационарному теплообмену получены для плоских поверхностей нагрева, находящихся в неподвижном жидком и сверхкритическом гелии. Измерения начинаются через $2(10)^{-5}$ секунды после мгновенного подвода мощности и проводятся для теплового потока в диапазоне от 0,05 до 20 Вт/см^2, для давления в пределах от 0,09 до 0,3

Мпаскаль при четырёх различных ориентациях нагревателя. Коэффициенты теплообмена для начального момента времени, ограниченные в первую очередь сопротивлением Капицы, в 10–100 раз превышают соответствующий коэффициент в стационарных условиях, а время установления стационарного состояния изменяется от 10^{-5} до 1 сек. Для теплового потока, не достигающего предельного значения, соответствующего пузырьковому кипению в стационарном состоянии, температура рассчитывается по формулам, справедливым для процесса чистой теплопроводности. При бóльших значениях потока наблюдается нестационарный процесс теплопроводности, приводящий к метастабильному характеру образования пузырьков, за которым следует переход к пленочному кипению.